CHAPTER 4

DESIGN OF THE REAR AXLE

Once the steering device has been designed, general geometry for rear axle subassembly must be designed. The present chapter contents go from theoretical knowledge in drive and suspension to specific elements design. Remembering the dynamic conditions the rear axle will be under while its performance, a vibrational analysis is included during steering action. Deflections and forces in assembly are got from this analysis, being important inputs for design process.

4.1 Types of drive and suspension

An important distinction between axles is whether a suspension is used as a steerable front axle or as a rear axle, and whether or not this contains the drive. A further distinction is drawn between rigid axles and independent wheel suspensions. The latter type include:

a) Double wishbone suspensions and
b) McPherson struts, which require only a little space at the side i.e. in the centre of the vehicle, making the steering angle possible.
c) Trailing link axles and semi-trailing link axles, which take up little vertical space, making it possible to have a wide boot with a flat floor, but which can have considerable diagonal springing.
d) Compound crank axle, an extremely space-saving component only fitted to front-wheel drive vehicles as the rear suspension.

In the case of rigid axles, the axle casing also moves over the entire spring travel. Due to that, space to be provided above this reduces the boot at the rear and makes it difficult to

house the spare wheel. Located at the front, the axle casing would be located (Reimpell, 1996[29])

4.2 Rigid axle

The advantages of using a rigid axle for the rear axle design are mainly:

a) It uses a minimum number of assembly parts.
b) Space saving, as suspension elements are fixed right on the rear axle and not in the ends of axle, attached to secondary elements that increase volume of vehicle.
c) Weight saving, if it is compared to additional mounting parts in case of crank axles.
d) No change to wheel camber when the body pitches during cornering, therefore there is constant lateral force transmission.
e) It is simple and economical to manufacture.
f) No changes to track width, toe-in and camber thus giving
g) Low tyre wear.

In the other hand, there are some disadvantages:

a) Mutual wheel influence (Fig.4.2)
b) Space requirement above the axle corresponds to the spring compression travel
c) Wheel load changes due to drive
d) Poor support basis b_{sp} for the body

4.2.1 Ratio of the wheel to the spring at reciprocal springing (fig 4.2).

It is defined by the following equation (Reimpell, 1996[30]):

$$i_{\varphi} = \frac{b_r}{b_{sp}} \tag{4.1}$$

Where b_r refers to distance between tires and b_{sp} refers to distance between springs. i_φ is a term that refers to rollingability of configuration.The greater the ratio, the less the roll reaction support of the body. It is illustrated in figure 4.1.

For our model it is

$$i_\varphi = \frac{b_r}{b_{sp}} = \frac{0.04m}{0.02m} = 2 \tag{4.2}$$

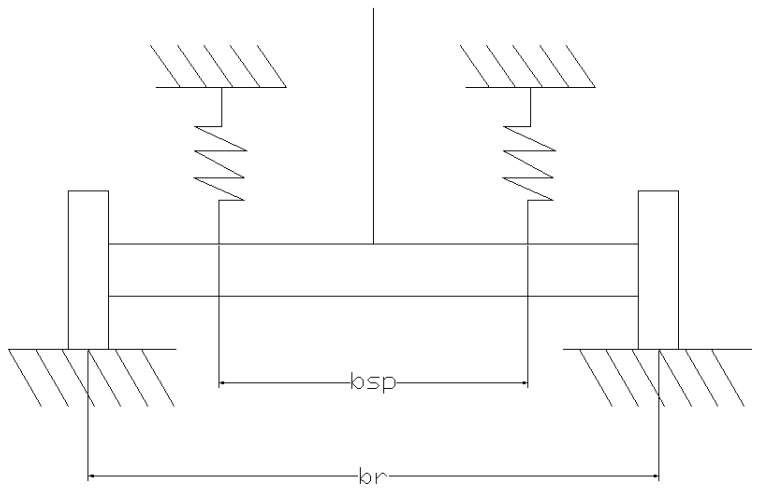

Figure 4.1 Ratio of wheel to spring.

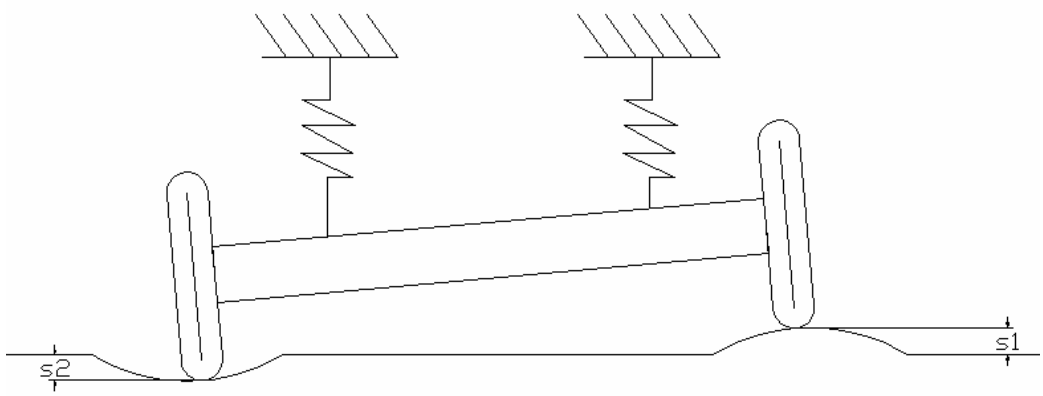

Figure 4.2 Reciprocal springing on rigid axle.

4.2.2 Distribution on rear axle

If passengers sit on a seat over the rear axle, on average 75% of their weight is carried on the rear axle (Reimpell,1996[31])

4.2.3 Conceptual design and selection

For rear axle design it will be developed a rigid axle according to the advantages previously mentioned and the readiness-to-be-used requirement in chapter 2. The following conceptual designs are to be compared.

a) I-beam rear axle.

Symmetry advantages are derived from the usage of an I-beam in the rear axle. Figure 4.3 and 4.4 show possible geometry for beam. Central kingpin rigidly attached to beam performs steering gyration axis. As shown in figure 4.3, extra tubular elements provide mounting place for bearings, hubs and wheels. Assembly of such elements is given by 2 keys located transversally to the tubular elements. Space for keys is shown in figure 4.4.

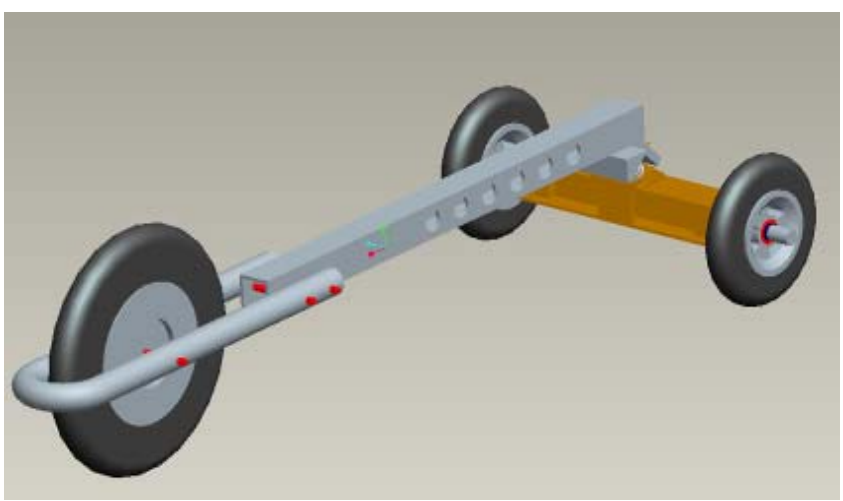

Figure 4.3 First conceptual design of structure

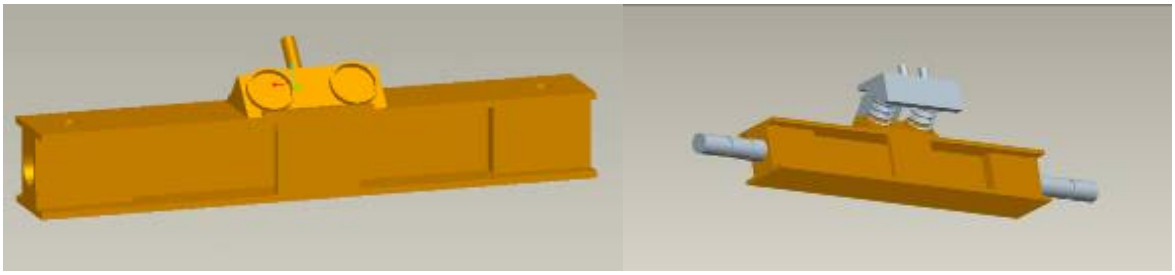

(a) (b)

Figure 4.4 (a) and (b) Sketch of rear axle

b) I-beam with 45° sloped tubular structure.

Under the same I-beam concept, this concept has a main difference: allocative bars at the ends of the beam are bended 45°. This adjustment provides the wheel a non-normal-to ground position, giving a better resistance to rolling effect. However, most wheels are set up to perform with a slight toe-in but not of 45°. Major benefits to be achieved with this set up are center- of- gravity lowering and better rolling resistance.

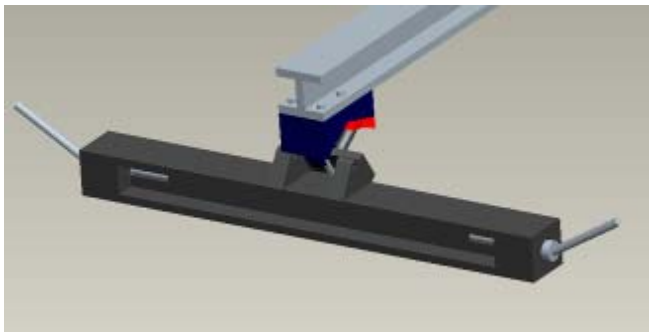

Fig.4.4 Second conceptual design of structure

c) Annular cross-section beam

As it is seen in figure 4.5, two cylinders will constitute the rear axle, one to give fixed support to the springs and the second where the wheels will be located. Annular profile reduces the amount of material and, in consecuence, the mass of the parts involved.

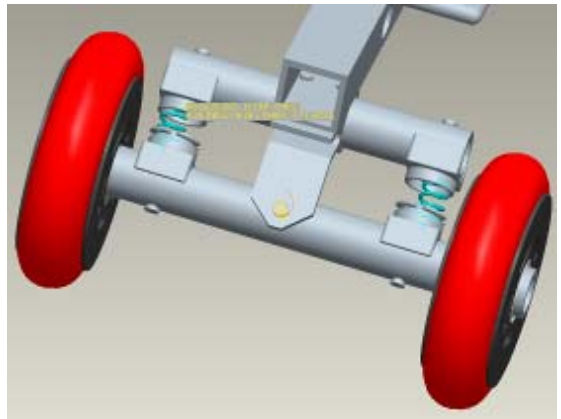

Figure 4.5 Third conceptual design of structure.

4.2.4 Selection of conceptual design

Consider chart 4.1.

Chart 4.1 Conceptual design decision matrix

Design	a)	b)	c)
No. of parts	8	10	9
Cross-section	I	I	Annular
Advantages	Cross section is used in automotive industry	Cross section is used in automotive industry	Material reduction and good torsion resistance
Maximum lenght [m]	0.06	0.08	0.04
Suggested b_r	0.06	0.08	0.04
Suggested b_{sp}	0.02	0.02	0.02
Rolingability i_φ	3	4	2

From the assembly quantity of parts, design a) has the least number of parts. Also it has a wheel ratio of 3. Furthermore, it has the advantage that the I cross section has been used widely in automotive industry (Reimpell, 1996[31]).

Design b) has 10 parts in its assembly, and as b), its cross section has been used in cars. This design has the highest wheel ratio, with a value of 4. However, the steering device it was based on is already discarded in chapter 3.

Basic consideration for selection is material reduction as well as security. From quoted studies in chapter 2, it is inferred that target market is not willing to carry an excessively heavy device as backpack. But security and steerability are also premises.

Being a weight-shifting-action activated device, it is desirable that rolling is promoted in design. So wheel ratio becomes a factor to consider. At low wheel ratios, rolling is highly promoted.

Design c) has the lowest wheel ratio with a value of 2. Also its cross section allows designer to reduce material in axle.

Transportability is an issue of major concern in weight and dimensions characteristics. A long axle will increase both, so an adequate maximum length should be set to avoid this problem.

In terms of steerability, transportability and material reduction, design c) gives better advantages than a).

For the present work design a) is the chosen conceptual design.

From these definitions the main tasks to be done are:

a) An analysis of the behavior of assembly, to find out the deflections the full set of springs undergo.

b) Design of the annular cross section beam under dynamic conditions with the previously calculated forces.

c) Design of the components shown in Chart 4.1

Chart 4.2 Elements to be designed

#	**Part**
1	Bearings
2	Short matrix bolts
3	Long matrix bolts
4	Spring support bolts
5	Steering kingpin

4.3 Analysis of the main beam under dynamic conditions

4.3.1 Analysis of assembly behavior

To find out the reaction forces on the 4-springs set a dynamic model of the suspension must be developed.

Consider diagram in fig. 4.4. Points A, B, C and D represent each of the points where springs contact the main beam, providing support on all the three wheel and steering effect on the rear axle. Each one with stiffness K_A, K_B, K_C, K_D, respectively. Recall the assembly geometrical and mass properties got from a computer analysis done in ProEngineer™ Wildfire in chart 4.2.

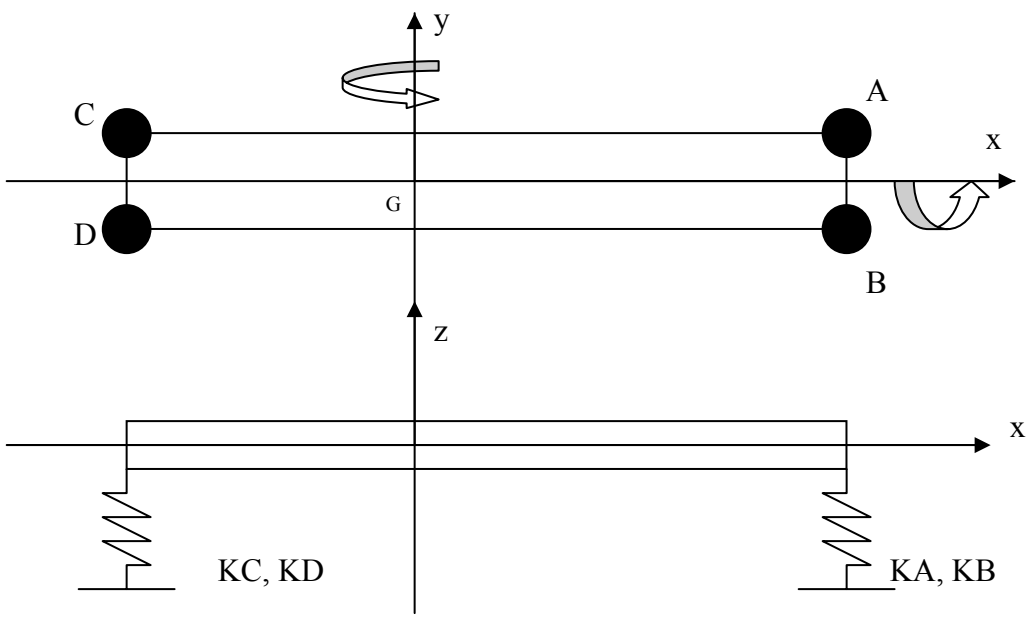

Fig. 4.4 Diagram for dynamic analysis of suspension springs.

	Rear axle	**Assembly**	**Assembly with driver**	**Units**
Volume	0.003	0.008	0.069	m^3
Surface area	0.585	1.492	3.022	m^2
Average density	921.384	1558.388	1595.250	kg/m^3
Mass	3.178	12.239	109.744	kg/m3
Moments of inertia (respect to center of gravity)				
Ixx	0.010	0.095	5.022	$kg.m^2$
Iyy	0.058	1.645	6.980	$kg.m^2$
Izz	0.062	1.681	9.297	$kg.m^2$
Radii of gyration (respect to principal axes)				
R1	0.056	0.088	0.214	m
R2	0.135	0.367	0.252	m
R3	0.139	0.371	0.291	m

Chart 4.2 Geometric and mass properties of assembly with and without rider.

Also reconsider the stiffness value got for steering springs in Chapter 3, page 59.

$$K=284111 \text{ N/m} \tag{4.3}$$

Stablishing all suspension springs to have stiffness K

$$K_A=K_B=K_C=K_D=K \tag{4.4}$$

And taking a typical damping ratio for springs (Reimpell, 1996[31])

$$e = 0.02 \tag{4.5}$$

A value for Z displacement damping coefficient is got

$$\varepsilon = \frac{C}{C_{cr}} = \frac{C}{2M_z\varpi_0} = 0.02 \tag{4.6}$$

Before the dynamic analysis, it is necessary to stablish the kinematic constraints for each spring, dependant of vertical displacement ZG, angular displacement in x axis and angular displacements in y axis.

$$Z_A = Z_G - L_x F \cdot \theta_y + L_y R \cdot \theta_x \tag{4.7}$$

$$Z_B = Z_G - L_x F \cdot \theta_y - L_y L \cdot \theta_x \tag{4.8}$$

$$Z_C = Z_G + L_x R \cdot \theta_y + L_y R \cdot \theta_x \tag{4.9}$$

$$Z_D = Z_G + L_x R \cdot \theta_y - L_y L \cdot \theta_x \tag{4.10}$$

A major assumption taken in these displacements expressions is small amplitude angular motion ($\theta_y < 15º; \theta_x < 15º$)

The suspension springs will be deflected a certain amount due to weight of assembly. Thus, z motions given above are relative to the static equilibrium position. This also means that the weight of the assembly will not appear in the force vector in the equation of motion.

Conservation of linear momentum: translation of center of mass

$$\sum F_Z = M_Z \cdot \ddot{Z} = -(F_A + F_B + F_C + F_D) + F_Z \tag{4.11}$$

Where

$$M_Z = 100kg$$

$$F_Z = -W_d$$

Conservation of angular momentum: rotations about Y axis –pitching motions

$$\sum Mom_y = I_Y \cdot \ddot{\theta}_y = -(F_A + F_B) \cdot L_x R + (F_C + F_D) \cdot L_x F + Mom_y \tag{4.12}$$

$$I_Y = I_y + M_z \cdot X_d^2 \tag{4.13}$$

$$Mom_y = -F_z \cdot X_d \tag{4.14}$$

Conservation of angular momentum: rotations about X axis –rolling motions

$$\sum Mom_y = I_x \cdot \ddot{\theta}x = (F_A + F_c) \cdot L_y L - (F_B + F_D) \cdot L_y L + Mom_x \tag{4.15}$$

$$I_X = I_x + M_z \cdot Y_d^2 \tag{4.16}$$

$$Mom_y = F_z \cdot Y_d \tag{4.17}$$

Matrix form of equations of motion is as follows:

$$I \cdot Z + C \cdot \dot{Z} + K \cdot Z = F \tag{4.18}$$

where

$$I = \begin{bmatrix} Mz & 0 & 0 \\ 0 & Ix & 0 \\ 0 & 0 & Iy \end{bmatrix} \quad K = \begin{bmatrix} Kzz & Kzx & Kzy \\ Kzx & Kxx & Kxy \\ Kzy & Kxy & Kyy \end{bmatrix} Z = \begin{bmatrix} Z_G \\ \theta_x \\ \theta_y \end{bmatrix} \text{ and F=} \begin{bmatrix} F_Z \\ Mom_x \\ Mom_y \end{bmatrix} \tag{4.19}$$

where Z and F are vectors of generic displacements and forces. Support springs are already deformed a certain amount due to the chassis weight, that´s why assembly weight does not appear in the equation of motion.

Elements of stiffness matrix are defined under two indexes. The first one is direction of generic force, and the second one, the direction of generic displacement.

$$K_{zz} = K_a + K_b + K_c + K_d \tag{4.20}$$

$$K_{zx} = L_{yR}(K_a + K_c) - L_{yL}(K_b + K_d) = 0 \tag{4.21}$$

$$K_{zy} = -L_{xF}(K_a + K_b) + L_{xR}(K_c + K_d) \tag{4.22}$$

$$K_{yy} = L_{xF}{}^2(K_a + K_b) + L_{xR}{}^2(K_c + K_d) \tag{4.23}$$

$$K_{xy} = L_{yR}(L_{xR}K_c - K_a L_{xF}) + L_{yL}(L_{xF}K_b - L_{xR}K_d) \tag{4.24}$$

$$K_{xx} = L_{yR}{}^2(K_c + K_a) + L_{yL}{}^2(K_b + K_d) \tag{4.25}$$

Numerical substitution of stiffness matrix gives

$$K = \begin{bmatrix} 1.136\text{E}6 & 0 & -256473 \\ 0 & 454.578 & 0 \\ -256473 & 0 & 313557 \end{bmatrix} \tag{4.26}$$

Solving for the undamped natural frequencies from the eigenvalue problem:

$$(K - I \cdot \lambda)\bar{a} = 0 \tag{4.27}$$

Mathematica™ gives the following results for the modal vectors and natural frequencies:

$$\varpi = \begin{bmatrix} 2.289 \\ 17.6972 \\ 29.7364 \end{bmatrix} \text{[rad/s]} \tag{4.28}$$

$$\Phi = \begin{bmatrix} 0.999397 & -0.03472 & 0 \\ 0 & 0 & 1 \\ 0.034715 & 0.999397 & 0 \end{bmatrix} \text{Modal vectors} \tag{4.29}$$

Three different damping coefficients are found then.

$$C_1 = 2\varepsilon M_z \varpi_{01} = 2(0.02)(109.744kg)(2.289/s) = 10.048kg/s \tag{4.30}$$

$$C_2 = 2\varepsilon M_z \varpi_{02} = 2(0.02)(109.744kg)(17.68/s) = 77.68kg/s \tag{4.31}$$

$$C_3 = 2\varepsilon M_z \varpi_{01} = 2(0.02)(109.744kg)(29.736/s) = 130.564kg/s \tag{4.32}$$

Each column represent one mode of response of the suspension system. Modes 1 and 2 present heaving (up/down) and pitching motions, and mode 3 presents pure rolling. Modal displacement response is shown in chart 4.2.2

	Mode		
Modal displacements	**1**	**2**	**3**
ZA	0.975	-0.734	0.02
ZB	0.975	-0.734	-0.02
ZC	1.008	0.214	0.02
ZD	1.008	0.214	-0.02

Chart 4.3 Modal displacement response for each spring.

Matrix equation in equation (41) is not an ordinary differential equation system, so the system must be solved by numerical methods. In this case the solution approach is a result of entering the system in Mathematica™. For the circular reference between Z displacement and rotation angle in y axis, maximum critical values for displacement and rotation are given. From the steering design maximum angle 5°, maximum z displacement is got from the substitution of the initial conditions

$$\begin{aligned} Z_{G0} &= 0 \\ \dot{Z}_{G0} &= 0 \\ \theta_y &= 5° \end{aligned} \tag{4.33}$$

For θ_y the solution is given under the following initial conditions

$$\begin{aligned} Z_G &= Z_{GMAX} \\ \dot{\theta}_y &= 0 \\ \theta_y &= 0 \end{aligned} \tag{4.34}$$

The solution of θx is easily found with the following initial conditions

$$\begin{aligned} \theta_x &= 0 \\ \dot{\theta}_x &= 0 \end{aligned} \tag{4.35}$$

Plotting in Mathematica™ the solution for each variable of vector

$$Z = \begin{bmatrix} Z_G \\ \theta_x \\ \theta_y \end{bmatrix} \tag{4.36}$$

The following plots are got:

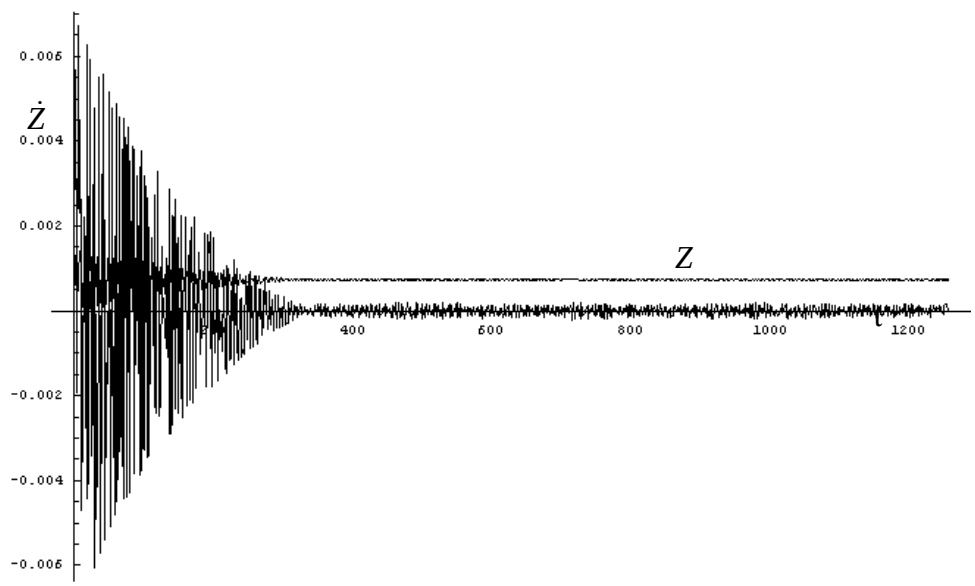

Figure 4.5 Displacement/velocity vs time plot for Z (first mode)

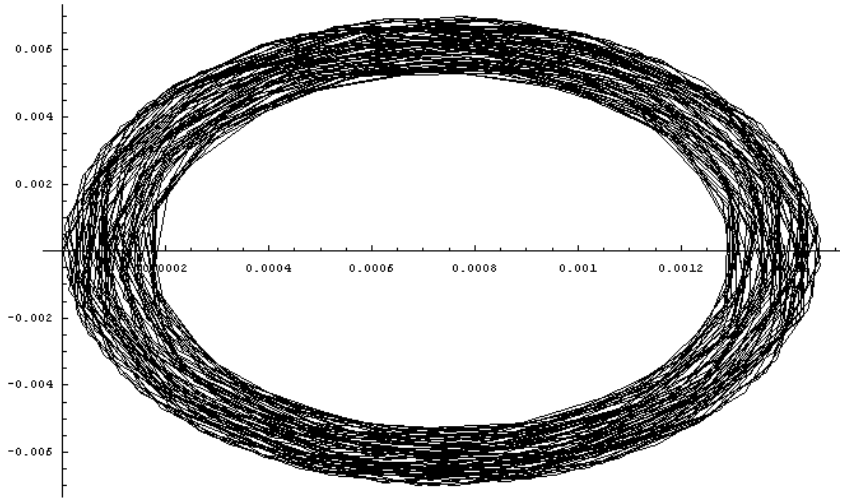

Figure 4.6 Displacement/velocity phase diagram for Z (first mode)

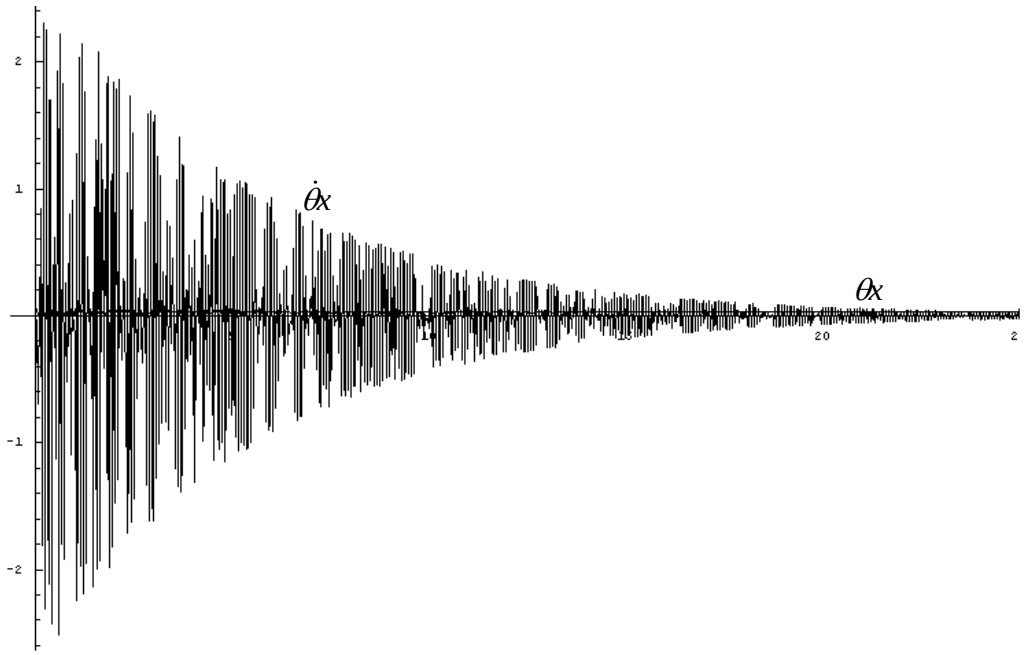

Figure 4.7 Angular displacement/ velocity vs time for rotation in x axis (first mode)

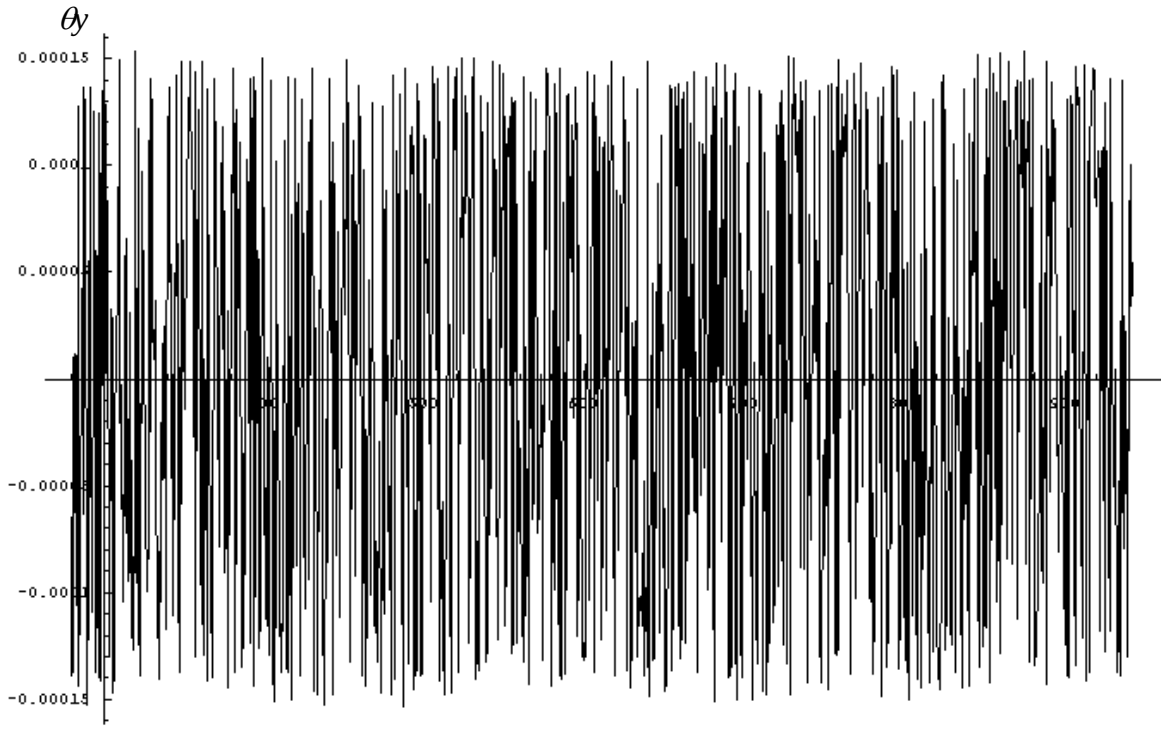

Figure 4.8 Angular displacement/ velocity vs time for rotation in y axis (first mode)

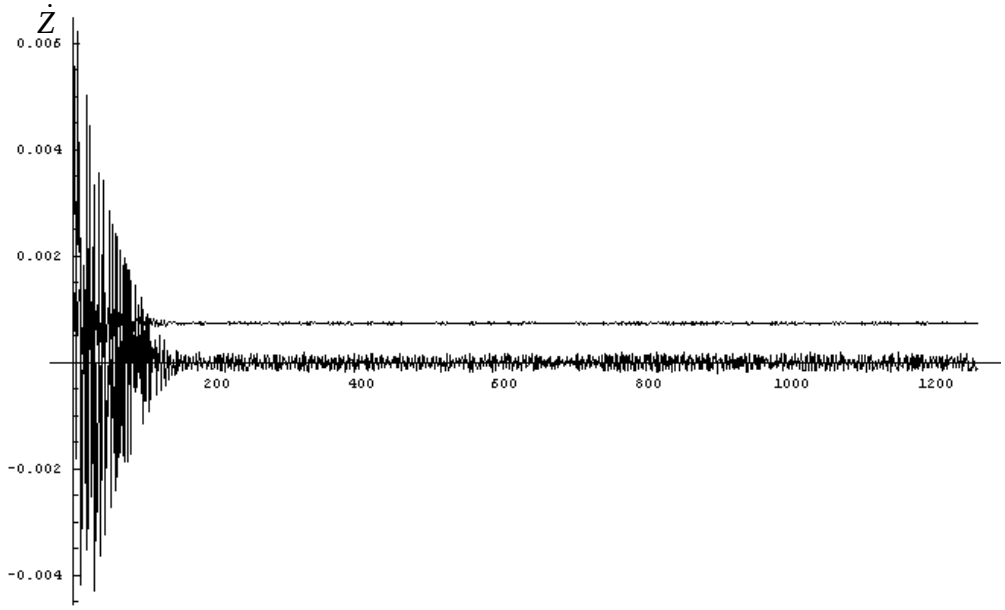

Figure 4.9 Displacement/velocity vs time plot for Z (second mode)

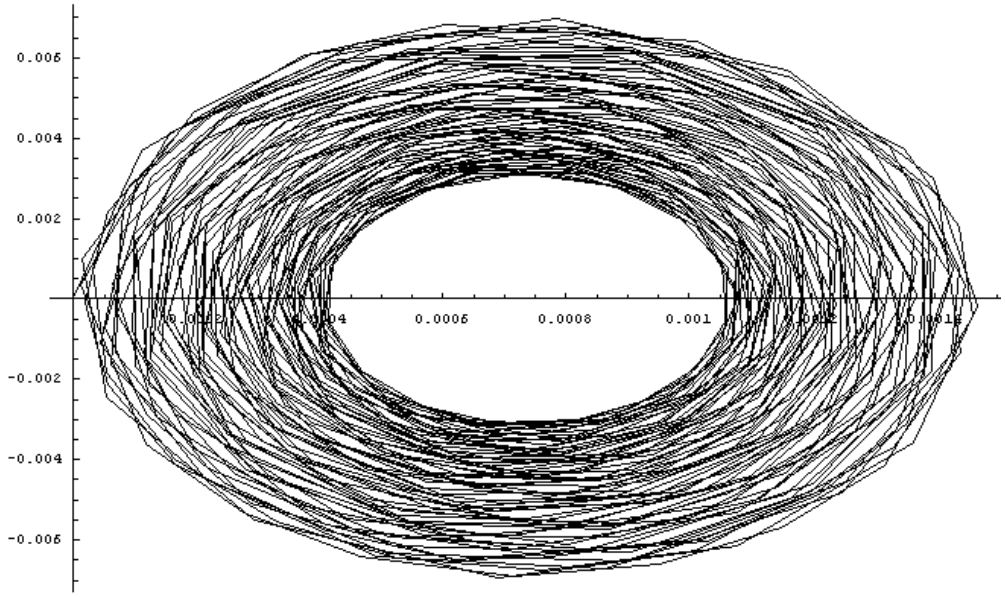

Figure 4.10 Displacement/velocity phase diagram for Z (second mode)

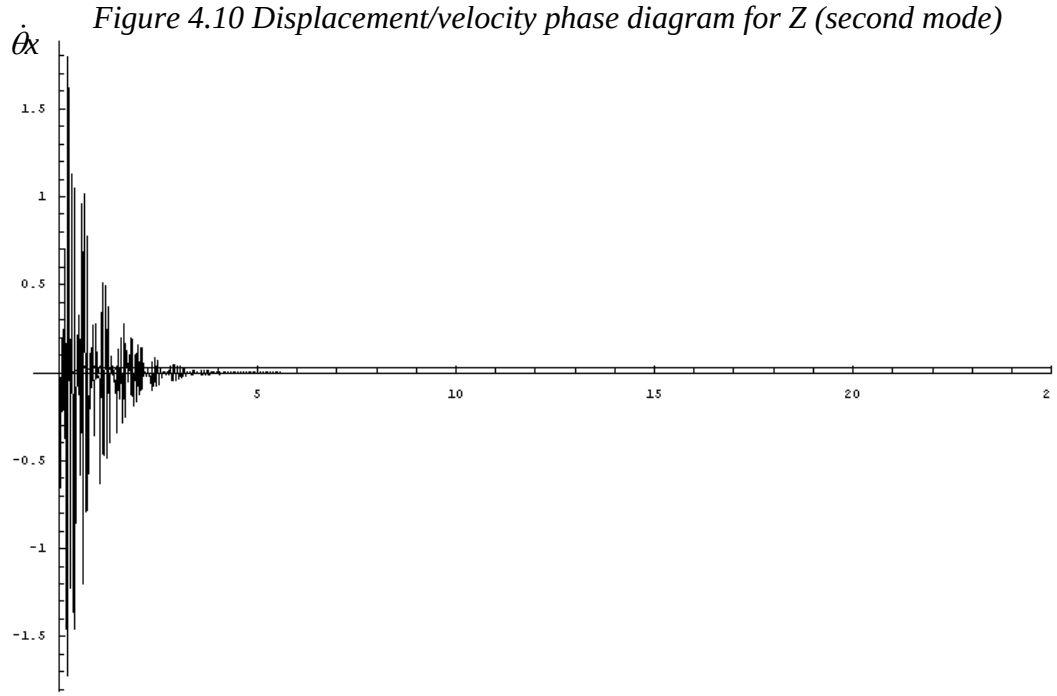

Figure 4.11 Angular displacement/ velocity vs time for rotation in x axis (second mode)

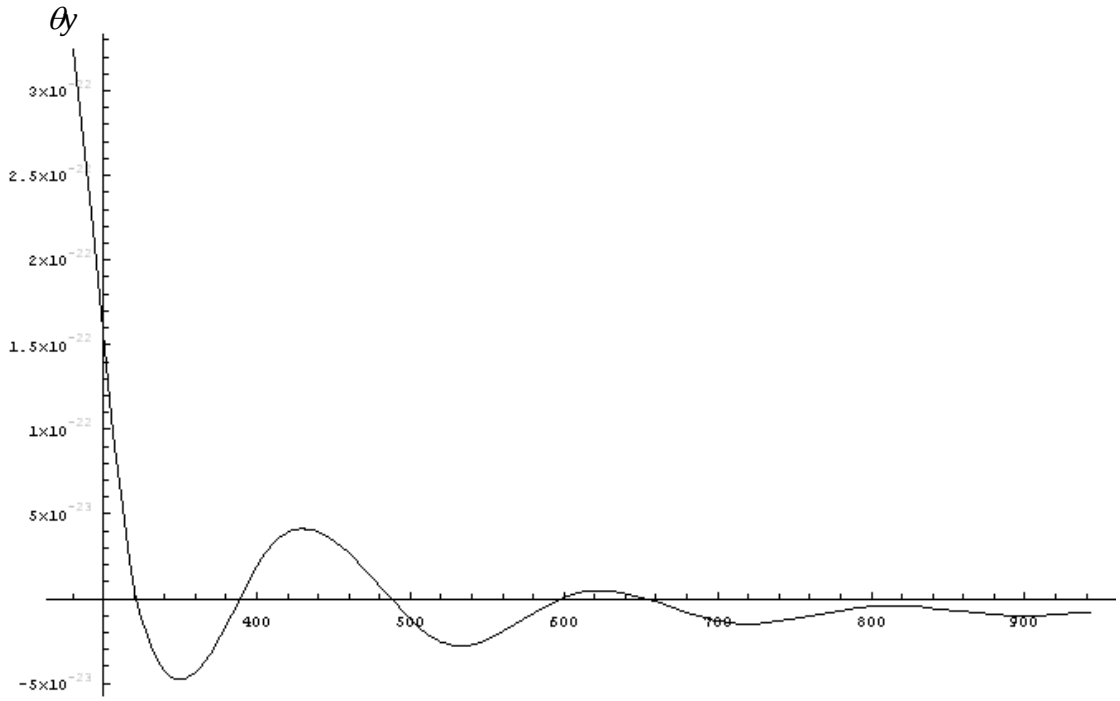

Figure 4.12 Angular displacement/ velocity vs time for rotation in y axis (second mode)

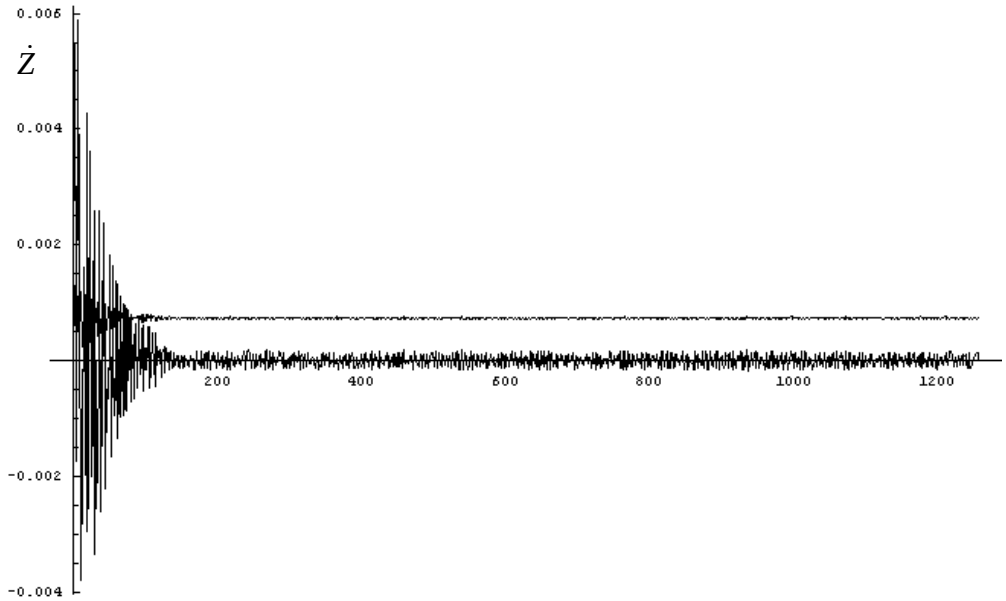

Figure 4.13 Displacement/velocity vs time plot for Z (third mode)

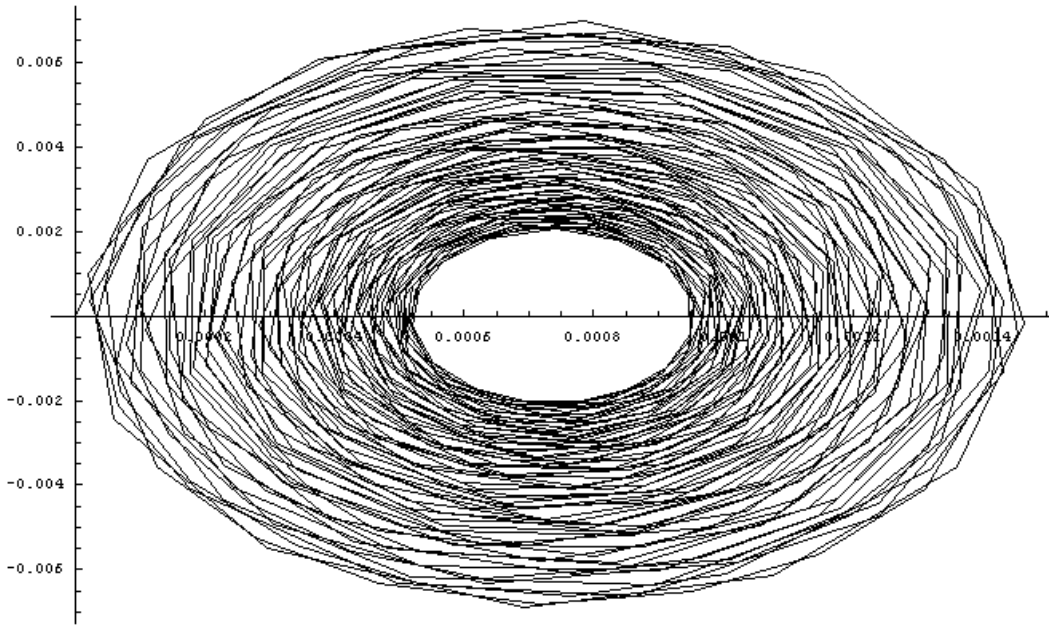

Figure 4.14 Displacement/velocity phase diagram for Z (third mode)

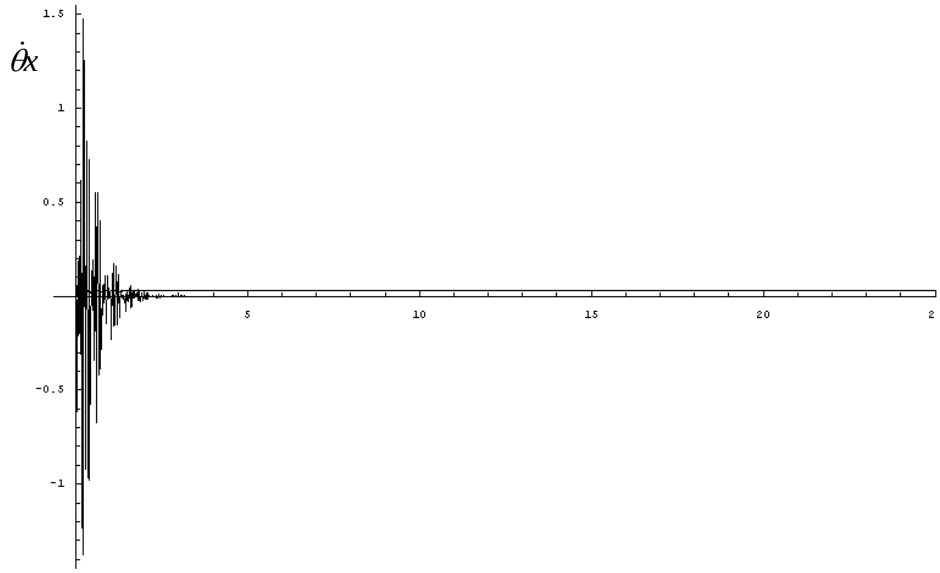

Figure 4.15 Angular displacement/ velocity vs time for rotation in x axis (third mode)

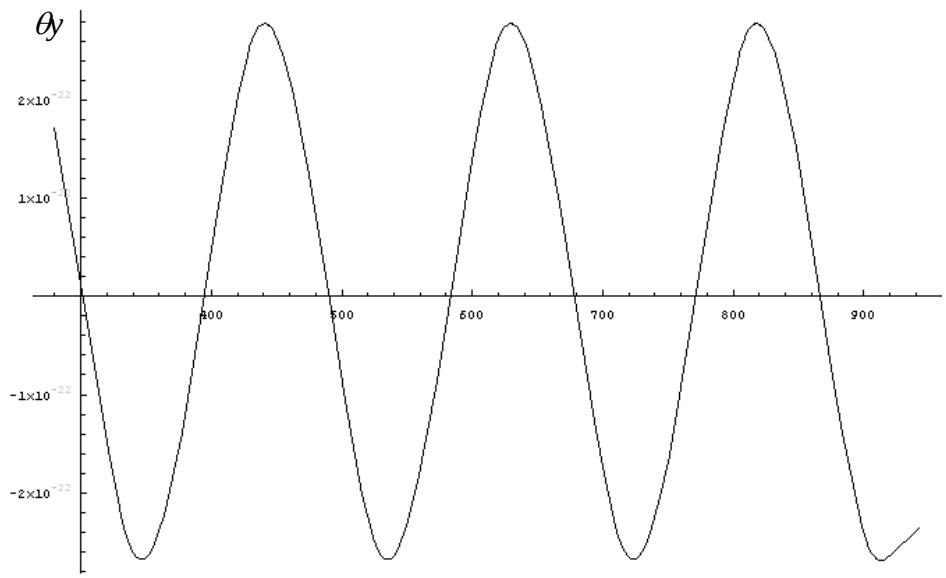

Figure 4.16 Angular displacement/ velocity vs time for rotation in y axis (second mode)

In figure 4.5, 4.9 and 4.13 it is observed that the maximum displacement Z_G undergoes is nearly 0.001 m and maximum velocity experimented is 0.007 m/s . Such displacement value becomes an input for kinematic constraints established in equation (30) to (33).

In figure 4.8, 4.12 and 4.16 angular displacement and angular velocity in y axis are plotted. As shown in those figures, maximum value for angular displacement and velocity are values of 10E-4 and 10E-22 order, that means 0.0001 rad and 1E-22 rad. Such values can be approximated to zero in the substitution of kinematic constraints.

In figure 4.7, 4.11 and 4.15 angular displacement and angular velocity in x axis are plotted. From those figures the maximum angular displacement value is 0.05 rad and maximum angular velocity is 2.2 rad/s.

Substitution of such values in kinematic constraints gives the data in chart 4.4

4.2.2 Behavior analysis of rear axle.

Spring analysis provides forces exerted on rear steering springs based on the premise that suspension springs connect total mass to ground being rear axle a fixed attachment. Such

Chart 4.4 Spring displacements

Point	Static spring deflection (m)	Maximum physical displacement [m]	Effective displacement [m]	Static force [N]	Operational dynamic force [N]	Effective force [N]	K=dF/dl [N/m]
Z_A	0.0009	0.002	0.0011	245.25	568.222	322.97	284111.012
Z_B	0.0009	0	-0.0009	245.25	0	-245.3	284110.985
Z_C	0.0009	0.002	0.0011	245.25	568.222	322.97	284111.012
Z_D	0.0009	0	-0.0009	245.25	0	-245.3	284110.985

model introduces some obstacles to develop a mathematic model. However, use of a dynamic finite element analysis is a good way to find out reaction forces and stress the rear axle undergoes. Chapter 6 presents results of analysis for displacements under dynamic conditions.

4.2.3 Design of components

4.2.3.1 Bearings.

Taking effective force value of 322.97 N (Chapter 4, page 88) pageand a mounting shoulder outer diameter of 0.04 m, a commercial catalogue must be consulted to find one that satisfies such requirements. For this effect SFK catalogues where consulted (SKF©, 2006[32]) shown in chart 4.5.

Specified dynamic load of 61808-2RZ bearing is 4940 N, so there is kept an extra range for load in design. Dealing with the mass issue, this bearing has 0.034 kg of weight, a reasonable amount to be added to total subassembly mass.

Further specifications of selected bearing are shown in figure 4.17.

Chart 4.5 SKF bearings catalogue

Deep groove ball bearings, single row										
Principal			Basic load ratings		Fatigue	Speed ratings		Mass	Designation	
dimensions			dynamic	static	load	Reference	Limiting			
					limit	speed	speed			
d	D	B	C	C0	Pu				* -SKF Explorer bearing	
mm			kN		kN	r/min		kg	-	
38,1	95,25	23,813	41	24	1,02	15000	11000	0,79	RMS 12	Aftermarket only
40	52	7	4,94	3,45	0,186	26000	16000	0,034	61808	
40	52	7	4,94	3,45	0,186	-	7500	0,034	61808-2RS1	
40	52	7	4,94	3,45	0,186	26000	13000	0,034	61808-2RZ	
40	62	12	13,8	10	0,425	24000	14000	0,12	61908	
40	62	12	13,8	10	0,425	-	6700	0,12	61908-2RS1	
40	62	12	13,8	10	0,425	24000	12000	0,12	61908-2RZ	
40	68	9	13,8	9,15	0,44	22000	14000	0,13	16008 *	
40	68	15	17,8	11,6	0,49	22000	14000	0,19	6008 *	
40	68	15	17,8	11,6	0,49	-	6300	0,19	6008-2RS1 *	
40	68	15	17,8	11,6	0,49	22000	11000	0,19	6008-2RZ *	
40	68	15	17,8	11,6	0,49	22000	11000	0,19	6008-2Z *	
40	68	15	17,8	11,6	0,49	-	6300	0,19	6008-RS1 *	
40	68	15	17,8	11,6	0,49	22000	14000	0,19	6008-RZ *	
40	68	15	17,8	11,6	0,49	22000	14000	0,19	6008-Z *	
40	68	21	16,8	11,6	0,49	-	6300	0,26	63008-2RS1	
40	80	18	32,5	19	0,8	18000	11000	0,37	6208 *	
40	80	18	35,8	20,8	0,88	18000	11000	0,34	6208 ETN9	
40	80	18	32,5	19	0,8	-	5600	0,37	6208-2RS1 *	
40	80	18	32,5	19	0,8	18000	9000	0,37	6208-2RZ *	
40	80	18	32,5	19	0,8	18000	9000	0,37	6208-2Z *	

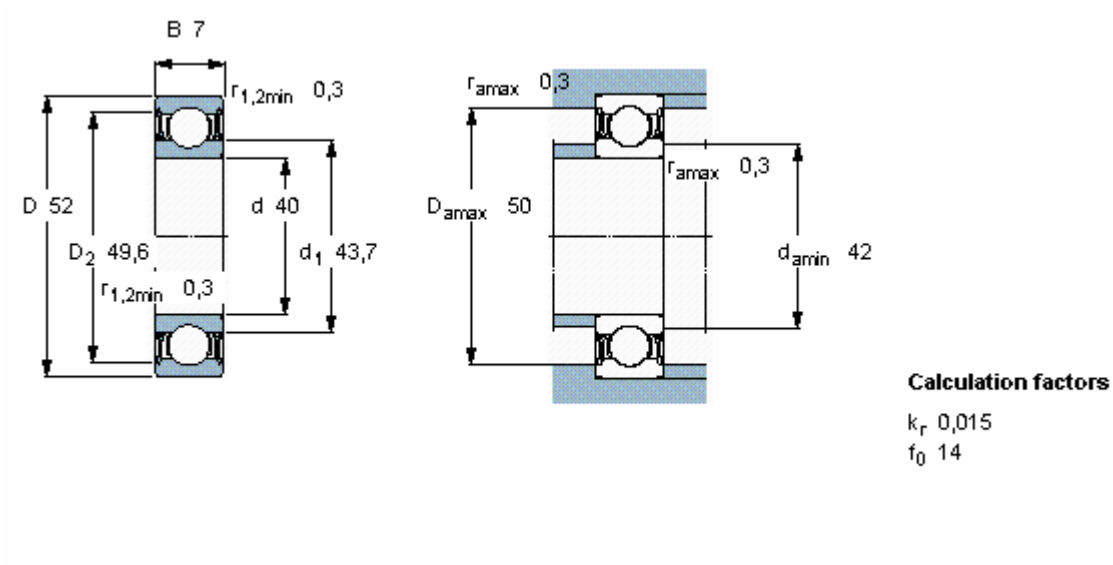

Figure 4.17 Specifications for 61808-2RZ bearing.

Bearing useful lifetime L_d is calculated as follows (Mott, 1996[33])

$$L_d = (C/P_d)^k (10^6) = \left(\frac{4940N}{568N}\right)^3 (10^6) = 6.578E8rev \tag{4.37}$$

where

C- dynamic load specification for bearing

P_d - design load (in this case, the biggest reaction in rear springs)

k= 14 (for SKF 61808-2RZ bearing)

Such value for expected lifetime can be translated to hours plotting the following function (Mott, 1996[34])

$$t_{hours} = \frac{L_d}{(rpm)\left(60\frac{\min}{h}\right)} \tag{4.38}$$

Plot is shown in figure 4.18

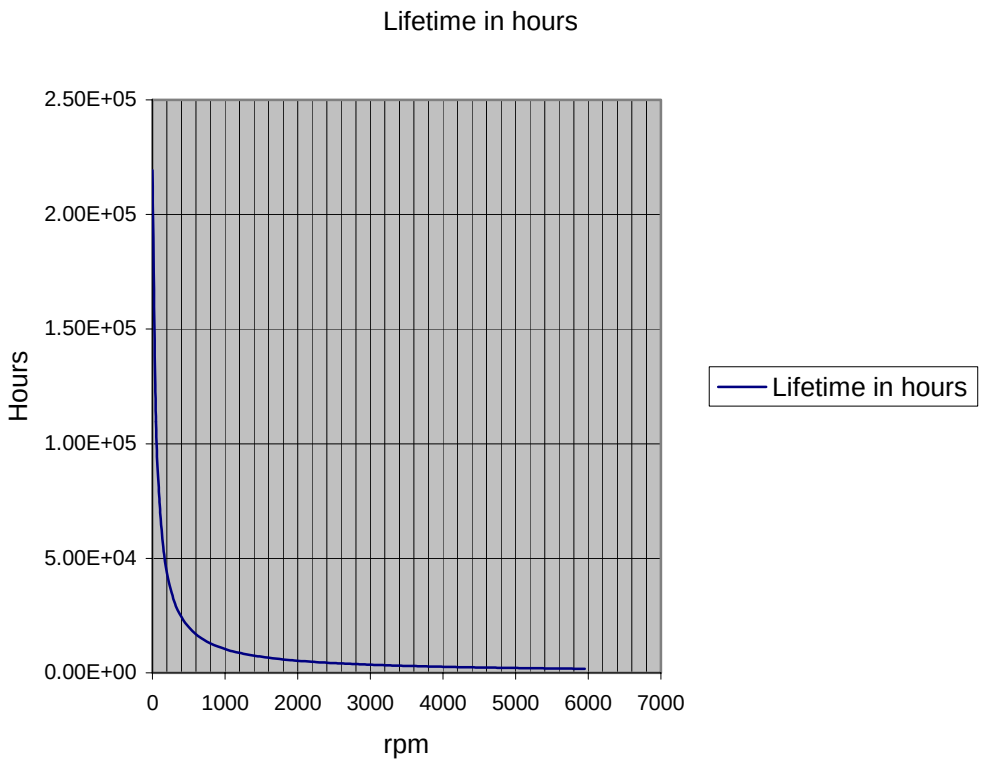

Figure 4.18 Lifetime plot in hours for selected bearing.

As the product will be used at low speeds, as indicated in chapter 2, it can be expected a lifetime of the order of 10E15.

4.2.3.2 Bolts and steering kingpin

Chart 4.6 shows dimensions and stress phenomena that each element is undergoing. Reported values for each element are given in next section.

Chart 4.6 Bolt elements for rear axle subassembly

#	Part	Length (m)	Trial Diameter (m)	Axial force	Shear force	Torsion
1	Short matrix bolts	0.02	0.01	Yes	Yes	Yes
2	Long matrix bolts	0.06	0.01	Yes	Yes	Yes
3	Spring support bolts	0.051	0.01	Yes	Yes	Yes
4	Steering kingpin	0.064	0.014	Yes	Yes	Yes

Elements are shown in figure 4.19.

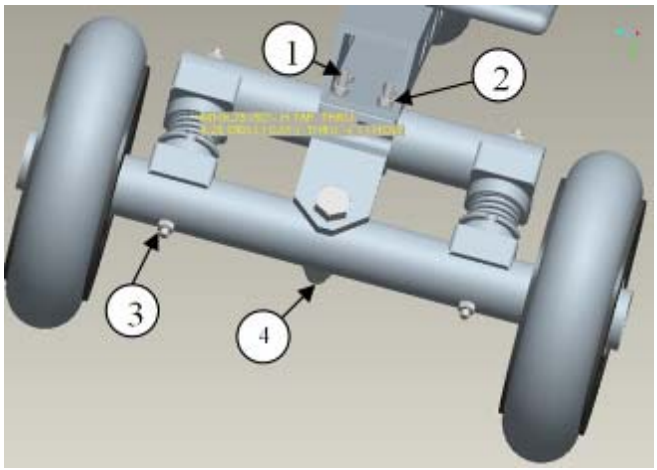

Figure 4.19 Bolts in rear axle.

Free body diagrams for elements are given in figure 4.20

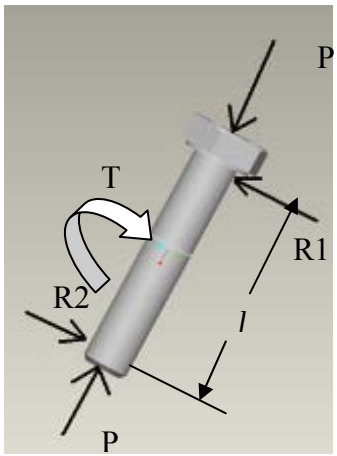

Figure 4.20 Free body diagram for bolt elements

All of these elements must be designed under dynamic premises. To achieve this, a trial diameter for each element is introduced. Chapter 6 concerns about dynamic effects on bolts elements. Working under Von Misses criteria –as the FEM analysis results are set up- a backward-working design procedure is followed. Using FEA advantages, from dynamic analysis in chapter 6, three main stresses are found: maximum principal stress,

minimum principal stress and intermediate principal stress (commonly known as maximum shear stress).

For bolts fixing spring supports, short and long bolts for subassembly mounting, it is got a value for their axial reaction force and principal stresses from chapter 6, in a first trial geometry using diameters shown in chart 4.6.

Such elements work under normal continuous inverse stress. Considering a design factor for dynamic performance N=4 (Mott, 1996[35]) and AISI 304 S30400 Stainless steel properties shown in chart 4.7 and 4.8.

Chart 4.7 Mechanical properties for AISI 304 S30400 stainless steel

	Metric	**English**
Hardness, Rockwell B	80	80
Tensile Strength, Ultimate	580 MPa	84100 psi
Tensile Strength, Yield	290 MPa	42100 psi
Elongation at Break	0.55 %	0.55 %
Modulus of Elasticity	193 GPa	28000 ksi
Izod Impact	150 J	111 ft-lb

Estimated endurance strength is determined from the following procedure (Mott, 1996[35]):

1. Yield strength S_y , from chart 4.8, has a value of 5.86E8 Pa. From chart 4.9, considering a turning process for bolts manufacturing, endurance strength of 2.75E8 Pa is found.

Chart 4.8 AISI 304 stainless steel properties and factors for design
AISI TYPE 304 S30400
Stainless steel (ground)

Su	586000000	Pa
Sy	276000000	Pa
Sn	275000000	Pa
Cs	1	
Cm	1	
Cst	0.8	
S'n	159500000	Pa

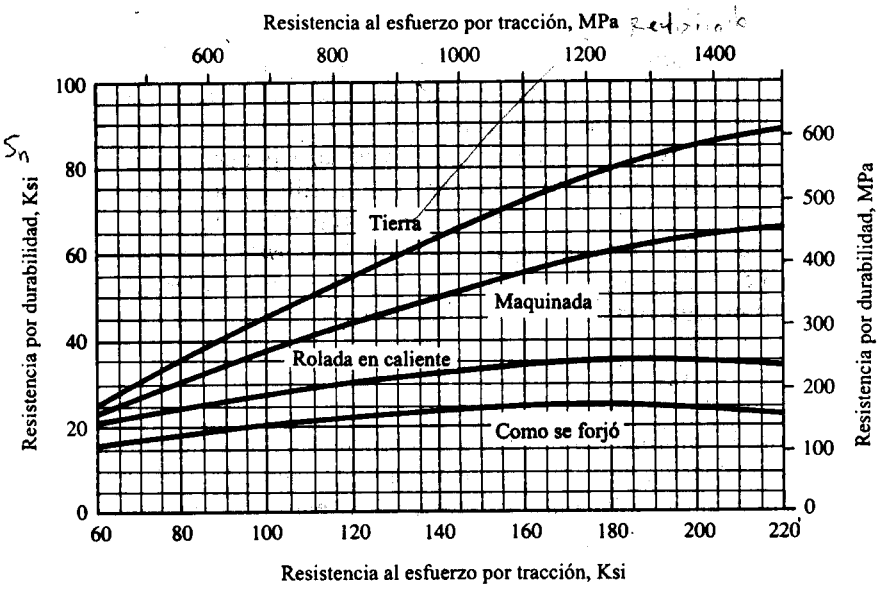

Chart 4.9 Endurance strength versus traction stress for stainless steel under various surface conditions (Mott, 1996)

2. Then values in chart 4.8 are substituted in the following equation.

$$S'_n = C_{st} C_m C_s S_n \tag{4.39}$$

Where

S'_n - Estimated endurance strength [Pa] (Mott, 1996[35])

C_{st} - Phenomena factor (0.8 axial tension, 0.58 torsion shear stress) (Mott, 1996[35])

C_s - Size factor (1.0 if diameter $\leq$ 0.01 m) (Mott, 1996[35])

C_m - Material factor (1.0 extruded steel) (Mott, 1996[35])

S_n - Endurance strength [Pa] (Mott, 1996[35])

Next set of equations show how design stress is determined and the force-area relation for normal stress (Mott, 1996[36]). N represents design factor, A cross sectional area and P axial force for free body diagram in figure 4.20.

$$\sigma_d = \frac{s'_n}{N} = \frac{1.595E8Pa}{4} = 3.9875E7Pa \tag{4.40}$$

$$\sigma_d = \frac{P}{A} \tag{4.41}$$

Design stress for AISI 304 stainless steel elements comes to a value of 3.9875E7Pa.

3. To define an adequate diameter for each bolt, some results referred to maximum principal stress, minimum principal stress and intermediate principal stress are got from dynamic FEA analysis. Such results are reported in chart 4.10.

Chart 4.10 Principal stresses for each element from dynamic analysis.

	Minimum principal [Pa]	**Maximum principal [Pa]**	**Maximum shear stress [Pa]**
Short bolt	1000000	3400000	1900000
Long bolt	55000	5800000	1700000
Spring support bolt	31000	3600000	1220000
Steering kingpin	19500000	52000000	37000000

Design under shear stress consideration is taken from the following expressions:

Maximum shear stress is given by the following expression (Gere, 2002[37])

$$\tau_{MAX} = \frac{4V}{3A} + \frac{Tr}{I_p} = \frac{4V}{3\left(\frac{\pi}{4}d^2\right)} + \frac{16T}{\pi \cdot d^3} \tag{4.42}$$

where

τ_{MAX} -Maximum shear stress experimented [Pa]

V - shear force, [N]

A - cross sectional area, [m^2]

T - torsion pair, [N· m]

I_p - polar moment of inertia $\left(\frac{\pi \cdot r^4}{2}\right)$ for round bars [m^4]

r - radius, [m]

d - trial diameter, [m]

Torque is determined from maximum axial force reported for bolts in chapter 6, P=450 N. Applying a lubrication factor K=0.2 (for completely dry surface) it comes in the following expression:

$T = KdP$

Solving for shear force V

$$V = \frac{3A}{4}\left(\tau_{MAX} - \frac{16T}{\pi \cdot d^3}\right) \tag{4.43}$$

where τ_{MAX} is taken from dynamic results for stress in bolts in chapter 6.

4. Taking τ_d to have design stress value of 3.9875E7 Pa, next equation is solved for d

$$\tau_d = \frac{4V}{3A} + \frac{Tr}{I_p} = \frac{4V}{3\left(\frac{\pi}{4}d^2\right)} + \frac{16T}{\pi \cdot d^3} \tag{4.44}$$

Traction area A_t is then calculated with such d value in the following equation

$$A_t = 0.7854(d - 0.9743p) \tag{4.45}$$

where p is thread pitch. Chart 4.10 shows results for such procedure.

Chart 4.11 Shear stress calculations for bolt diameters.

	Short matrix bolts	**Long matrix bolts**	**Spring support bolts**	**Steering kingpin**
Trial diameter [m]	0.01	0.01	0.01	0.014
A [m^2]	7.854E-05	7.854E-05	7.854E-05	1.539E-4
K [-]	0.2	0.2	0.2	0.2
Reported P [N]	450	450	450	450
T [N m]	0.9	0.9	0.9	1.26
Reported t_{MAX}	1900000	17000000	12200000	37000000
V [N]	158.0807617	731.3826583	448.6393195	4078.923468
t_d	39875000	39875000	39875000	39875000
Recalculated d [m]	0.005322386	0.00691157	0.006147993	0.01283357
Metric Standard	M6	M6	M6	M14
Traction A [m^2]	2.22486E-05	3.75183E-05	2.96863E-05	0.000129355

Trial diameters come to an adequate value over the required diameter *d* required for the experienced shear force. As a design decision, diameter for first three bolts was standarized to 0.006 m (M6), that is the closest value to the required diameter. For steering kingpin, diameter was standardized to M14, a 0.014 m diameter.

In the same way, axial reactions were got from dynamic analysis and recalculated diameters were got and they are shown in chart 4.12. Evaluation procedure is as follows:

1. Dynamic axial reactions are got from chapter 6.
2. From (63) an expression of cross-sectional area in terms of axial force and axial stress is got

$$A = \frac{P}{\sigma_d} \tag{4.46}$$

3. Recalculated diameter values are got and then compared with trial diameter in chart 4.12.

Chart 4.12 Axial force calculations for bolt diameters.

#	Part	S_d [Pa]	Dynamic Maximum axial reaction P [N]	Recalculated Area [m^2]	Recalculated Diameter [m]	Next Standard
1	Short matrix bolts	39875000	1.52E-08	3.81E-16	2.20E-08	M3
2	Long matrix bolts	39875000	1.64E-07	4.11E-15	7.24E-08	M3
3	Spring support bolts	39875000	1.24E-08	3.12E-16	1.99E-08	M3
4	Steering kingpin	39875000	1.67E-07	4.13E-15	7.27E-08	M3

As it can be seen, required diameter for axial stress considerations is smaller than the one required for shear stress considerations. For this work final configuration for elements is present in chart 4.13.

Chart 4.13 Final configuration for bolt elements.

#	Part	Standard	Length [m]
1	Short matrix bolts	M6	0.03
2	Long matrix bolts	M6	0.055
3	Spring support bolts	M6	0.055
4	Steering kingpin	M14	0.07

4.2.3.4 Conduits

Chosen material for conduits is aluminum 6061, which fatigue strength is 6.29E7 Pa, taken from chart 4.11.

Chart 4.14 Mechanical properties of aluminum 6061 (matweb.com)

	Metric	English
Hardness,	30	30

Brinell		
Ultimate Tensile Strength	124 MPa	18000 psi
Tensile Yield Strength	55.2 MPa	8000 psi
Elongation at Break	25 %	25 %
Elongation at Break	30 %	30 %
Modulus of Elasticity	68.9 GPa	10000 ksi
Ultimate Bearing Strength	228 MPa	33100 psi
Bearing Yield Strength	103 MPa	14900 psi
Poisson's Ratio	0.33	0.33
Fatigue Strength	62.1 MPa	9000 psi
Machinability	30 %	30 %
Shear Modulus	26 GPa	3770 ksi
Shear Strength	82.7 MPa	12000 psi

Consider free body diagram of rear axle conduit in figure 4.19. 813 N force corresponds to total force in axle got in dynamic analysis, page 88. Shear force equation and bending moment equation for free body diagram in figure 4.21 under symmetry condition are:

$$\Sigma F_y = R_A - 813N + V = 0 \tag{4.47}$$

$$\Sigma M_o = R_A x - 813 \cdot (x - 0.1m) - M = 0 \tag{4.48}$$

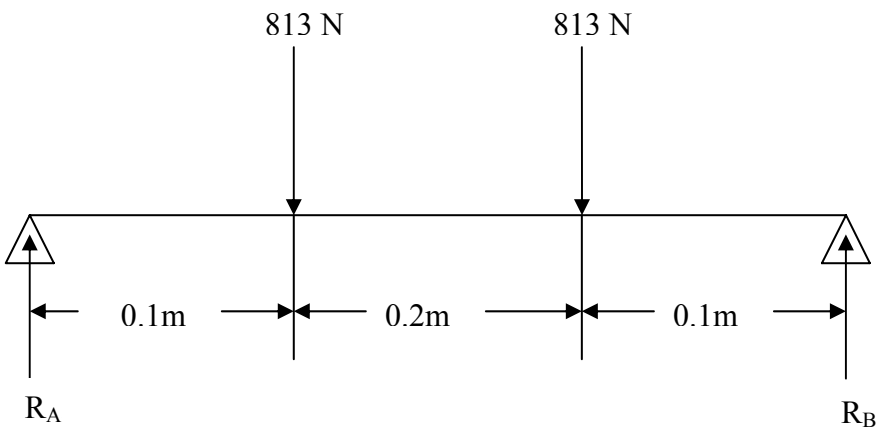

Figure 4.20 Free body diagram for rear axle conduit

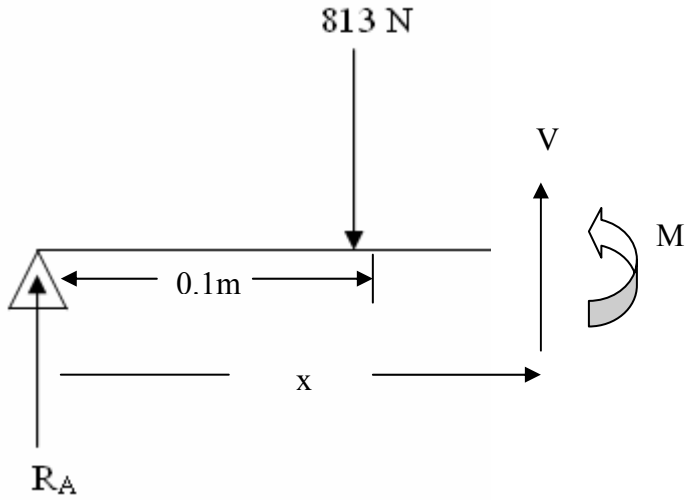

Figure 4.21 Free body diagram for symmetry condition.

Shear force diagram is shown in figure 4.20 and moment diagram in figure 4.21.

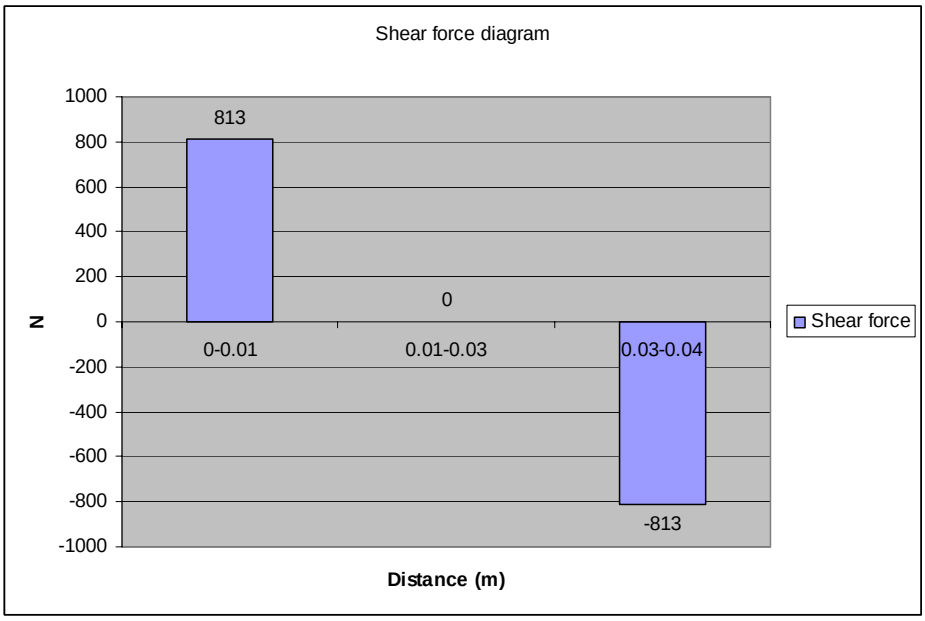

Figure 4.21 Shear force diagram for rear axle

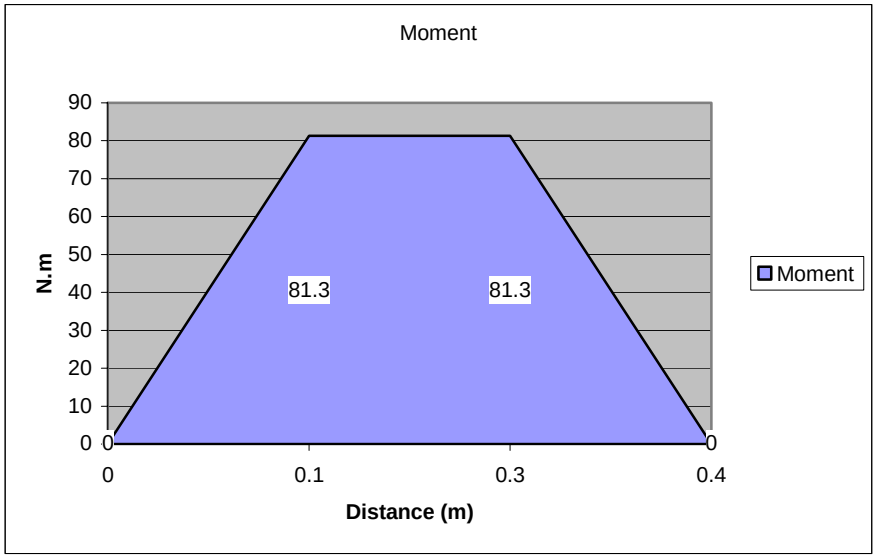

Figure 4.22 Moment diagram for rear axle

Maximum bending moment is 8.13 N.m . Given moment of inertia I , and setting inner diameter to be 0.75 times the outer diameter it is set

$$I = \frac{\pi}{64}\left[d_2^4 - (0.75d_2)^4\right] = 0.03356d_2^4 \tag{4.49}$$

Section modulus S is got from

$$S = \frac{I}{c} = \frac{0.03356d_2^4}{0.5d_2} = 0.06712d_2^3 \tag{4.50}$$

Required section modulus is got by

$$S = \frac{M_{MAX}}{\sigma_{ALLOW}} = \frac{8.15N.m}{62.1E6Pa} = (1.3124\text{E-}06)m^3 \tag{4.51}$$

$$S = 0.06712d_2^3 = (1.3124\text{E-}06)m^3$$

Equaling the two last expressions

$$d_2 = \sqrt[3]{\frac{(1.3124\text{E-}06)m^3}{0.06712}} = 0.035m \tag{4.52}$$

(4.53)

As shown, an adequate external diameter for conduits is 0.035 m and an inner diameter of 0.026 m.

Diameter evaluation will be extended to matrix conduit for FEA effects.

Area related with such inner and outer diameter values is

$$A = \frac{\pi}{4}\left(d_2^2 - d_1^2\right) = 4.31\text{E - }04m^2 \tag{4.54}$$

From trade sizes in chart 4.11, the closest area value to the required one is 1 ¼ size.

Chart 4.12 Trade sizes for aluminum conduit (republic-conduit.com)

Trade size [in]	**d_2 [m]**	**d_1 [m]**	**A [m^2]**
1/2	0.02134	0.0158	0.000162
1/4	0.02667	0.02093	0.000215
1	0.0334	0.02664	0.000319
1 1/4	0.04216	0.03505	0.000434

4.3 Rear axle set of parts

Full list of parts in module 1 subassembly are listed in chart 4.12

No.	**Part**
1	Rear axle conduit
2	Matrix conduit
3	Steering kingpin
4	Rear tire
5	Spring support
6	Adjuster
7	Rear hub
8	Bearing
9	M6x55 Bolts
10	M6 nut
11	Steering matrix
12	M14 nut
13	Spring
14	M6x30 bolts
15	M6x55 Bolts

16	Seat
17	Main beam
18	Front wheel conduit support
19	Front tire
20	Front hub
21	M10x0.156

Chart 4.13 Parts list

Overview of module 2 subassembly is shown in figure 4.22.

4.3.1 Fitting

Parts 1, 2, 5,6 and 11 have hole features that must be given a certain fitting. Needed fitting for such features (identified by indicated tolerances in technical drawings) is *running or sliding clearance fit* (Mott, 1996[38]). Such fittings were got from chart 4.13 and are indicated in technical drawings in appendix 4.

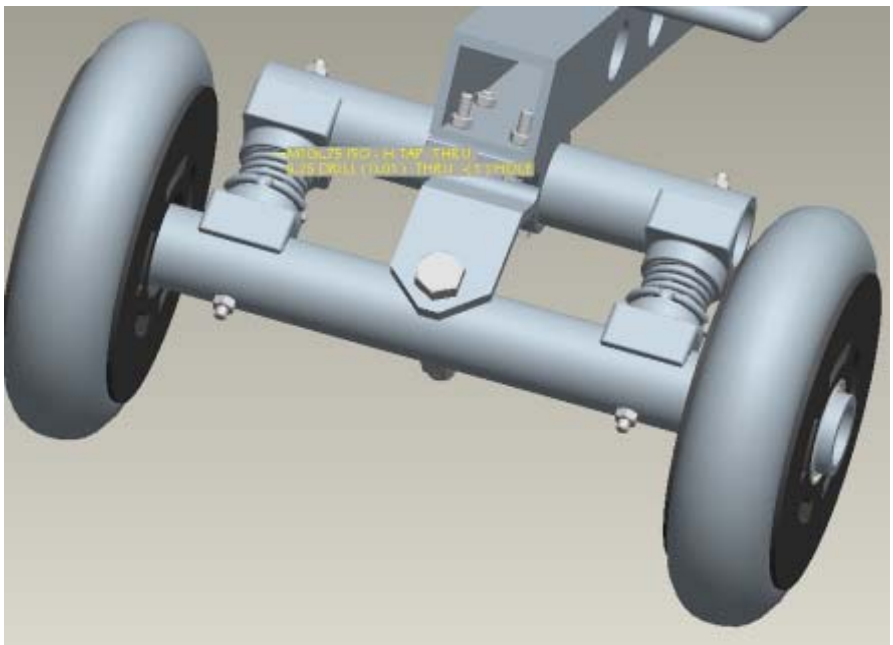

Figure 4.22 Overview of module 1 subassembly.

For every hole feature indicated in drawings, RC8 fit was chosen since it allows considerable clearance, so it allows to use trade parts with as-received tolerances.

4.3.2 Manufacture

Parts 1, 2, 5, 6 and 11 are to be constructed in a milling and/or turning machine. For this purpose, appendix 4 presents the technical drawings for their construction.

4.3.3 Trade parts

Trade parts are included in appendix 2, with their respective vendors.

4.3.4 Assembly plan

Assembly plan is shown in appendix 3 with illustrations, descriptions and numbered steps, as well as required tools for such effect.

Chart 4.14 Running fit chart (Mott, 1996)

Rango de tamaño nominal (")	Clase RC2			Clase RC5			Clase RC8			Rango de tamaño nominal (")
	Límites de holgura	Límites estándar		Límites de holgura	Límites estándar		Límites de holgura	Límites estándar		
Base		Orificio	Eje		Orificio	Eje		Orificio	Eje	Hasta
0–0.12	0.1 0.55	+0.25 0	−0.1 −0.3	0.6 1.6	+0.6 −0	−0.6 1.0	2.5 5.1	+1.6 0	−2.5 −3.5	0–0.12
0.12–0.24	0.15 0.65	+0.3 0	−0.15 −0.35	0.8 2.0	+0.7 −0	−0.8 −1.3	2.8 5.8	+1.8 0	−2.8 −4.0	0.12–0.24
0.24–0.40	0.2 0.85	+0.4 0	−0.2 −0.45	1.0 2.5	+0.9 −0	−1.0 −1.6	3.0 6.6	+2.2 0	−3.0 −4.4	0.24–0.40
0.40–0.71	0.25 0.95	+0.4 0	−0.25 −0.55	1.2 2.9	+1.0 −0	−1.2 −1.9	3.5 7.9	+2.8 0	−3.5 −5.1	0.40–0.71
0.71–1.19	0.3 1.2	+0.5 0	−0.3 −0.7	1.6 3.6	+1.2 −0	−1.6 −2.4	4.5 10.0	+3.5 0	−4.5 −6.5	0.71–1.19
1.19–1.97	0.4 1.4	+0.6 0	−0.4 −0.8	2.0 4.6	+1.6 −0	−2.0 −3.0	5.0 11.5	+4.0 0	−5.0 −7.5	1.19–1.97
1.97–3.15	0.4 1.6	+0.7 0	−0.4 −0.9	2.5 5.5	+1.8 −0	−2.5 −3.7	6.0 13.5	+4.5 0	−6.0 −9.0	1.97–3.15
3.15–4.73	0.5 2.0	+0.9 0	−0.5 −1.1	3.0 6.6	+2.2 −0	−3.0 −4.4	7.0 15.5	+5.0 0	−7.0 −10.5	3.15–4.73
4.73–7.09	0.6 2.3	+1.0 0	−0.6 −1.3	3.5 7.6	+2.5 −0	−3.5 −5.1	8.0 18.0	+6.0 0	−8.0 −12.0	4.73–7.09
7.09–9.85	0.6 2.6	+1.2 0	−0.6 −1.4	4.0 8.6	+2.8 −0	−4.0 −5.8	10.0 21.5	+7.0 0	−10.0 −14.5	7.09–9.85
9.85–12.41	0.7 2.8	+1.2 0	−0.7 −1.6	5.0 10.0	+3.0 0	−5.0 −7.0	12.0 25.0	+8.0 0	−12.0 −17.0	9.85–12.41

Nota: los límites se dan en milésimas de pulgada.
Fuente: ANSI Standard B4.1—1967 (revisión 1979), *Preferred Limits and Fits for Cylindrical Parts* (American Society of Mechanical Engineers, Nueva York).